17th World Conference on Earthquake Engineering, 17WCEE
Sendai, Japan - September 13th to 18th 2020

DEEP LEARNING-BASED SITE CLASSIFICATION BY MICROTREMOR H/V SPECTRAL RATIO

H. Miura[(1)], D. Miyashita[(2)], T. Kanno[(3)], M. Shigefuji[(4)], T. Abiru[(5)]

[(1)] *Associate Professor, Hiroshima University, hmiura@hiroshima-u.ac.jp*
[(2)] *Undergraduate Student, Hiroshima University, b165666@hiroshima-u.ac.jp*
[(3)] *Professor, Kyushu University, kanno@arch.kyushu-u.ac.jp*
[(4)] *Assistant Professor, Kyushu University, shigefuji@arch.kyushu-u.ac.jp*
[(5)] *General Manager, The Chugoku Electric Power Co. Inc., 368753@pnet.energia.co.jp*

Abstract

This study introduces deep learning techniques for automatic site classification and estimation of time-averaged shear-wave velocity in upper 30m depth (Vs30) from observed microtremor horizontal-to-vertical spectral ratio (MHVR). The observed MHVRs at K-NET and KiK-net stations in Japan are analyzed. We confirm clear correlations between the predominant periods in the observed MHVRs and NEHRP site classes (B, C, D and E). Deep learning-based neural network architectures are developed for estimating the site classes and Vs30s from the MHVRs. The result for the site classification shows that the accuracies for class B and E are higher than 70% and overall accuracy reaches 65%. The Vs30s predicted by the deep learning approach show good agreement with the observed Vs30s.

Keywords: site class, Vs30, microtremor H/V spectral ratio, deep learning, neural network

1. Introduction

Time-averaged shear-wave velocity in upper 30m depth (Vs30) has been used for evaluating site effects in strong ground motion prediction equations (GMPEs) and specifying site classes in building codes. PS-logging data is basically required for obtaining Vs30 value at borehole site. However, it is difficult to collect the Vs30s over a wide area because of the limitation of borehole and PS-logging data. Recently Vs30 mappings have been extensively performed in various regions by using geological, topographical and/or geomorphological data [e.g., 1, 2]. Whereas such proxy-based Vs30 maps would be useful for strong ground motion mapping, estimation accuracy of the Vs30 at a specific site would not be always high because of the spatial change of the site conditions within a mesh of the map.

Microtremors, i.e., ambient vibrations of surface grounds, have been widely used for site characterizations because they can be observed anywhere and at any time. In particular, the horizontal-to-vertical (H/V) spectral ratio technique has been used to evaluate predominant periods of the grounds. Recently microtremor H/V spectral ratio (MHVR) has been applied for estimating Vs structure from inversion analysis based on surface wave theory [3] or diffuse field theory [4]. However, additional information such as surface wave dispersion data and/or soil profile is still required for accurate Vs profiling from MHVRs [4-6]. If Vs30 value or site class at the observation site can be estimated directly from observed MHVR, detailed evaluation of site amplifications would be accomplished for accurate ground motion prediction.

Recently deep learning and artificial intelligence solutions has been dramatically developing in the various fields of science and engineering [e.g., 7]. In this study, deep learning technique for automatic site classification from observed MHVR is introduced. The observed MHVRs at K-NET and KiK-net stations in Japan, are analyzed for estimating their NEHRP site classes (B, C, D and E). First the characteristics of the MHVRs in each site class are examined. Data augmentation is performed by providing artificial white noise to the MHVRs. Neural network architectures are developed by optimizing the given training data in a neural network software. The optimized model is applied to the validation data for automatic site classification and estimation of Vs30 values. The accuracies of the deep learning-based predictions are discussed.

2. Vs30 Data and Microtremor H/V Spectral Ratios

In this study, we analyze Vs30 data and MHVRs observed at K-NET and KiK-net seismic observation stations in Japan developed by National Research Institute for Earth Science and Disaster Resilience (NIED) because S-wave velocity (Vs) profiles derived from PS-logging surveys are available at these stations. Vs30 values are calculated from the Vs profiles from the Eq. (1),

$$Vs30 = \frac{30}{\sum_{i=1}^{n} H_i / Vs_i} \tag{1}$$

here, H and Vs indicate thickness and shear-wave velocity in layer i, respectively, and n means the number of the layers up to 30 m depth. Since the depths of Vs profiles at the K-NET stations are shallower than 20m, the Vs30 values at the K-NET stations are estimated from average shear-wave velocity at the deepest layer and the empirical equations developed by Midorikawa and Nogi [8].

Microtremor data observed by the authors [9-11] are analyzed in this study. The MHVRs at the K-NET and KiK-net stations were obtained from the Fourier spectra for horizontal and vertical components as follows,

$$MHVR(f) = \frac{\sqrt{FS_{NS}(f)^2 + FS_{EW}(f)^2}}{FS_{UD}(f)} \tag{2}$$

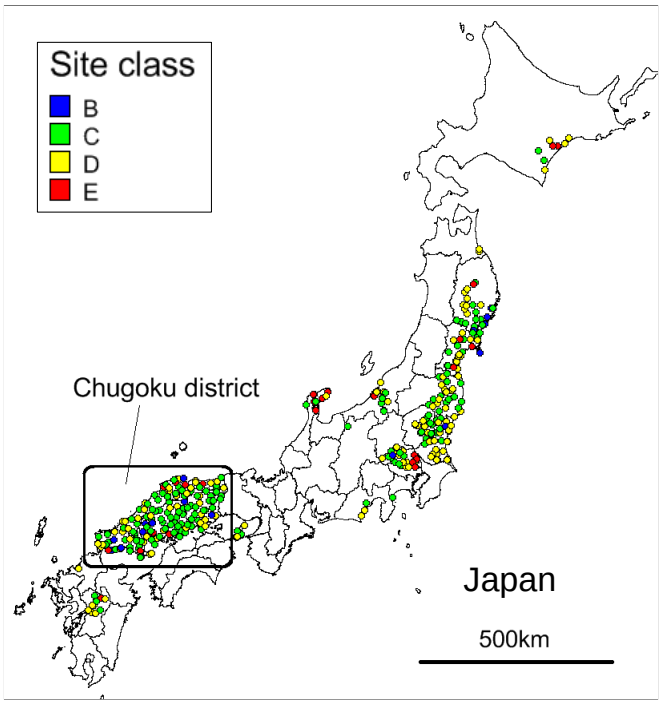

Fig. 1 – Locations of target seismic stations of K-NET and KiK-net, Japan

Table 1 – Number of MHVR and Vs30 data analyzed in this study

Site class	Vs30(m/s)	Num. of data
B	760<Vs30≦1500	19
C	360<Vs30≦760	170
D	180<Vs30≦360	129
E	Vs30≦180	29
Total		347

here, *f* and *FS* indicate frequency and Fourier spectrum of the observed microtremor, respectively. The subscripts *NS*, *EW* and *UD* mean north-south, east-west, and up-down components, respectively. The Fourier spectra were smoothed by the Parzen window with the bandwidth of 0.5Hz. Figure 1 shows the distribution of the target sites in this study. Almost 50 % of the target stations are concentrated in Chugoku district, western part of Japan. The colors of the figure indicates the NEHRP site class B-E derived from the Vs30s. Table 1 shows the number of MHVRs in each site class. Totally 347 MHVR and Vs30 data are analyzed in this study.

Figure 2 shows the obtained MHVRs for each site class. Gray and solid black lines indicate the MHVRs at each observation station and their mean values, respectively. Broken lines show the range of the standard deviation of the MHVRs in each class. The MHVRs of class B show almost no peak or small peaks in the frequency higher than 10 Hz. The MHVRs of class C mostly show moderate peaks between 3 - 10 Hz and the mean peak frequency of 7 Hz. The mean peak frequency in the MHVRs of class D is approximately 2 - 3 Hz and the largest standard deviation is found in this class. Predominant peaks are found in the MHVRs of class E at around 1 Hz, suggesting strong impedance contrast in the Vs structures beneath the sites. These results indicate that the shapes and predominant periods in the MHVRs almost correspond to the Vs30 values, and suggest the possibility of automatic site classification from the MHVRs.

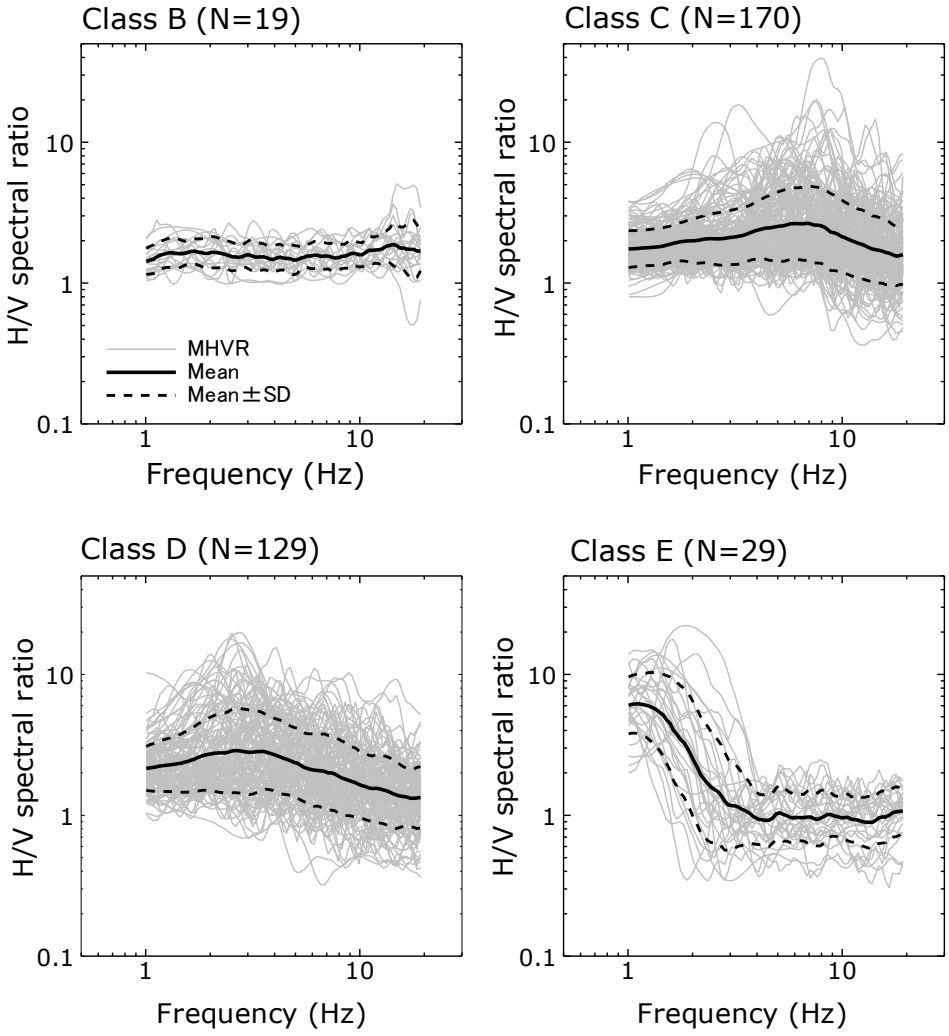

Fig. 2 – Microtremor H/V sapectral ratios observed at each NEHRP site class

3. Deep Learning-based Site Classification

Since large number of training data is required for accurate deep learning-based estimation, data augmentation is performed to the MHVRs to increase the number of training data. Random values for each frequency of the site class with the amplitude of 50 % of the standard deviation of the MHVRs are given to the MHVRs in the data augmentation. Totally 1000 MHVRs including such artificially created data for each site class are prepared for deep learning. The target frequency is 1 to 10 Hz. Although MHVR data at frequencies lower than 1 Hz would be useful for accurate site classification, the MHVRs are contaminated by noise in such lower frequencies at some of the stations probably due to weak amplitude response of the sensor at the lower frequencies used in the observations. The MHVR data is resampled by providing constant frequency interval in common logarithmic scale. Totally 81 points of the MHVR at each station are analyzed in following steps.

Recently artificial intelligence solutions have been dramatically developing in various fields of science and engineering. Deep learning (DL), one of machine learning techniques, has been recognized as the most suitable approach in automatic detection, identification and classification of big data. Thus we apply the DL technique for site classification from MHVRs. The DL structure consists of neural network modeled by

multiple layers such as nonlinearity layer, affine layer and fully connected layer. The input data is trained by the neural network to find the best solution from backpropagation of given training data. Numerous layer structures can be considered for the site classification. We use Neural Network Console [12] developed by SONY because the software can find the best solution by automatically creating possible structures. First we classify 80 % of the MHVRs including the augmented data as training data and the rest 20 % as validation data. Then the DL model is developed based on the training data, and the classification accuracy is assessed for the validation data.

Figure 3 shows the neural network structure developed for site classification. One dimensional array (N=81) is given as input data. In the model, Parametric Rectified Linear Unit (PReLU) [13] is applied in nonlinearity layer to normalized the input data and to activate positive trend of the data. Dropout [14] is adopted to suppress overfitting by removing randomly selected neurons with the probability of 0.5 at the training stage. The Affine layer provides weight factors to the normalized data. The normal Rectified Linear Unit (ReLU) [7] is also applied in the second nonlinearity layer and another Affine layer is given. Batch Normalization [15] is employed in fully connected layer to suppress overfitting and accelerating convergence speed. Finally the backpropagation is performed to minimize the Huber loss [16] between the given correct answer and the estimated value, and to find the best solution for accurate site classification. Figure 4 shows the learning

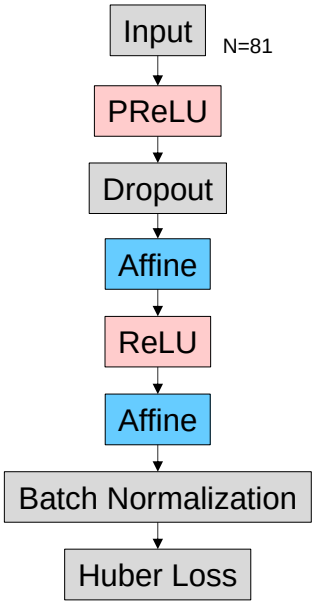

Fig. 3 – Neural network structure for site classification

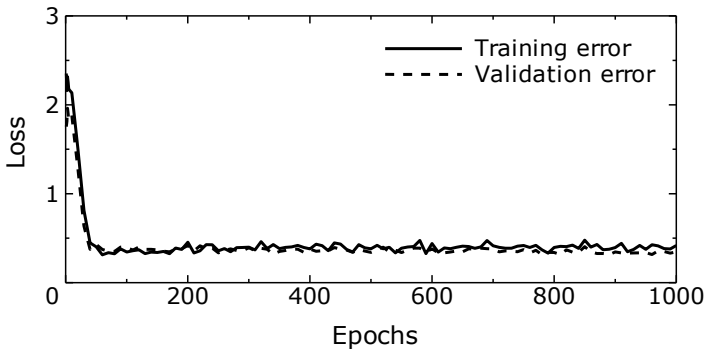

Fig. 4 – Loss functions in learning process of site classification

Table 2 – Accuracy assessment of validation data in DL-based site classification

		Estimated				Recall
		B'	C'	D'	E'	
Truth	B	153	55	0	0	0.74
	C	61	122	21	0	0.60
	D	10	86	75	11	0.41
	E	0	0	34	170	0.83
Precision		0.68	0.46	0.58	0.94	
				Overall accuracy		0.65

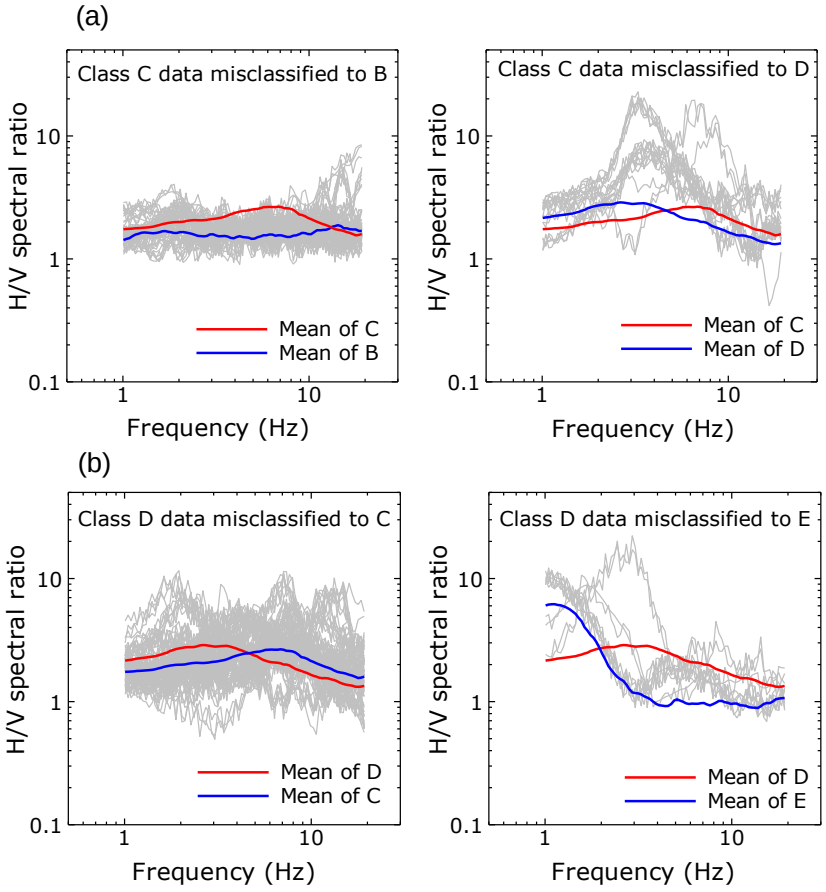

Fig. 5 – MHVR data misclassified in DL-based sica classification

process of the developed DL model. Epoch indicates the number of learning passes for all training samples. We select the number of Epochs at 1000 because we confirmed that the smallest loss functions are found not only for the training data but also the validation data, indicating that overfitting is successfully suppressed by the adopted model.

Table 2 shows the result of the site classification for the validation data. Totally 200 MHVR data is classified for each site class. Recall and precision indicate fractions of total amount of relevant samples that are actually retrieved, and fractions of relevant samples among the retrieved samples, respectively. Overall accuracy is defined as a ratio of correctly classified samples to a total amount of samples. Approximately 70 %

of the site B data and more than 80 % of the site E data are correctly classified by the DL model. On the contrary, the classification accuracies for the site C and D data are around 60 %. The overall accuracy is 65 %. The accuracy in this study is slightly lower than that in the previous preliminary analysis [11] in spite that the number of training data is increased. This would probably be because that the MHVRs in this study lack the data in the lower frequency range between 0.5-1 Hz due to the sensor specification used in the observation as shown above. Figure 5 (a) and (b) represents the MHVR data of Class C and D mis-classified by the model, respectively. Since the shapes of the MHVRs are very similar to the mean value of the mis-classified site class, it is difficult to accurately identify the site class from the MHVRs.

4. Deep Learning-based Estimation of Vs30

It would be beneficial to estimate Vs30 values directly from MHVR for evaluating site effects in GMPEs. Thus we examine a possibility of automatic estimation of Vs30 from MHVR using the DL technique. The DL model is developed by analyzing the training and validation data used in the previous chapter. Figure 6 shows the neural network architecture developed by the Neural Network Console for estimating Vs30 values. In this model, first Dropout is performed to the input data. The Swish function [17] is applied in the nonlinearity layer, and the Affine layer is employed to provide the weight factors. The pair of Hyperbolic Tangent (Tanh) function [18] and the Affine layer is applied to the data. Figure 7 shows the learning curves for the training and

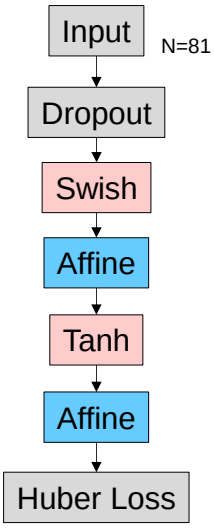

Fig. 6 – Neural network structure for Vs30 estimation

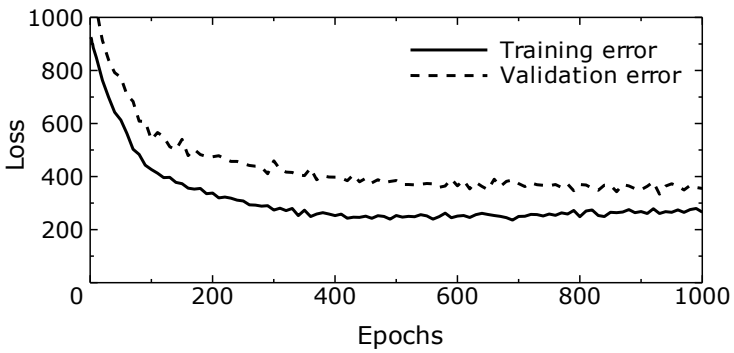

Fig. 7 – Loss functions in learning process of Vs30 estimation

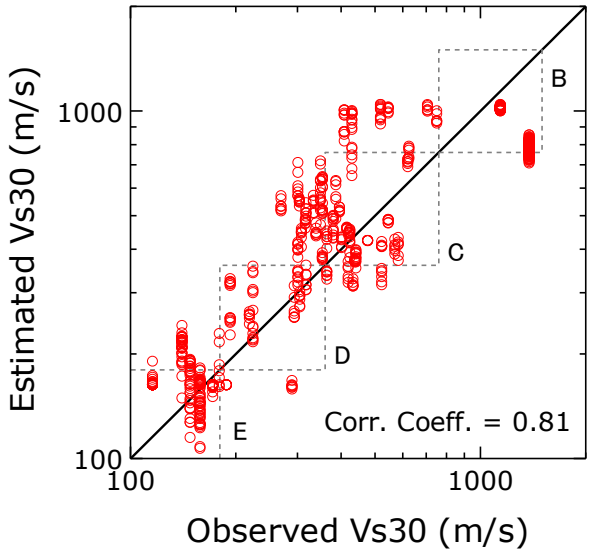

Fig. 8 – Relationship between observed Vs30s and estimated Vs30s

validation data. We confirm that the loss functions are successfully converged in the learning process by 1000 Epochs.

Figure 8 shows the relationship of the Vs30s between the observed and the estimated values for the validation data. Regions with broken lines represent the areas of the site classes. Since the number of data for the class B is limited, the estimation accuracy especially for larger Vs30 data is not high. However, the estimated Vs30s are highly correlated to the observed values in total. The correlation coefficient of the Vs30s is approximately 0.81. The result shows that the developed DL model accurately produces Vs30 from the observed MHVRs. In order to improve the accuracies of the site classification and the Vs30 estimation, it is necessary to increase the number of training data and to expand the frequency range in the MHVRs lower than 1 Hz.

5. Concluding Remarks

This study introduced the deep learning techniques for automatic site classification and Vs30 estimation from the observed MHVR. The MHVRs and Vs30s at totally 347 seismic stations of K-NET and KiK-net in Japan were analyzed. We found that the MHVRs at NEHRP site class B show almost no predominant peak or small peak at frequency higher than 10 Hz, the MHVRs at class C show moderate peaks at around 7 Hz, the MHVRs at class D show larger peaks at around 3 Hz, and the MHVRs at class E show strong peaks at around 1 Hz. The DL architectures were modeled by the Neural Network Console including the nonlinearity layers, the Affine layers and the backpropagation. The result of the site classification showed that approximately 65 % of the data were correctly classified by the DL model. The estimated Vs30s by the DL model were correlated to the observed Vs30. We confirmed the applicability of the DL technique for automatic site classification and Vs30 estimation from MHVRs. In order to improve the accuracy, it is necessary to increase the number of training data and to include the MHVR data at frequencies lower than 1 Hz in the analysis.

6. Acknowledgements

The shear-wave velocity profiles at K-NET and KiK-net stations disclosed by National Research Institute for Earth Science and Disaster Resilience (NIED) are used in this study.

7. References

[1] Allen TI, Wald DJ (2009): On the use of high-resolution topographic data as a proxy for seismic site conditions (Vs30), *Bull. Seism. Soc. Am.* **99** (2A), 935-943.

[2] Wakamatasu K, Matsuoka M (2013): Nationwide 7.5-arc-second Japan engineering geomorphologic classification map and Vs30 zoning, *Journal of Disaster Research*, 8(5), 904-911.

[3] Arai H, Tokimatsu K (2004): S-wave velocity profiling by inversion of microtremor H/V spectrum, *Bull. Seism. Soc. Am.* **94** (1), 53-63.

[4] Sánchez-Sesma FJ (2017): Modeling and inversion of the microtremor H/V spectral ratio: physical basis behind the diffuse field approach, *Earth, Planets and Space*, **69**:92, doi.org/10.1186/s40623-017-0667-6.

[5] Tumurbaatar Z, Miura H, Tsamba T (2019): Site effect assessment in Ulaanbaatar, Mongolia through inversion analysis of microtremor H/V spectral ratios, *Geosciences*, **9** (5), 228, doi.org/10.3390/geosciences9050228.

[6] Miura H, Fujita H, Su Su Than K, Hibino Y (2019): Estimation of site response during the 2016 Chauk, Myanmar earthquake based on microtremor-derived S-wave velocity structures, *Soil Dynamics and Earthquake Engineering*, **126**, 105781, doi.org/10.1016/j.soildyn.2019.105781.

[7] LeCun Y, Bengio Y, Hinton G (2015): Deep learning, *Nature*, 521(7553), 436-444.

[8] Midorikawa S, Nogi Y (2015): Estimation of Vs30 from shallow velocity profile, *Journal of Japan Association for Earthquake Engineering*, **15**(2), 91-96 (in Japanese with English abstract).

[9] Kanno T, Miura K, Kumagai C (2008): Accuracy verification of estimation method for predominant period of ground at earthquake observation points in Chugoku district, *Butsuri-Tansa*, **61**(6), 533-543 (in Japanese with English abstract).

[10] Nogi Y, Midorikawa S, Miura H (2016). Site classification by microtremors and preliminary analysis of site amplification during strong shaking for difference site classes, *J. Struct. Const. Eng.* 723, 843–850 (in Japanese with English abstract).

[11] Miura H, Midorikawa S (2019). Deep learning-based site classification by microtremor H/V spectral ratio, *Summaries of Technical Papers of Annual Meeting, Architectural Institute of Japan*, II, 515-516 (in Japanese).

[12] SONY (2019): *Neural Network Console Ver. 1.6.0*, https://dl.sony.com/app/.

[13] He K, Zhang X, Ren S, Sun J (2015): Delving deep into rectifiers: Surpassing human-level performance on ImageNet classification, arXiv:1502.01852.

[14] Srivastava N, Hinton G, Krizhevsky A, Sutskever I, Salakhutdinov R (2014): Dropout: A simple way to prevent neural networks from overfitting, *Journal of Machine Learning Research*, 15, 1929-1958.

[15] Ioffe S, Szegedy C (2015): Batch normalization: Accelerating deep network training by reducing internal covariate shit, arXiv:1502.03167v3.

[16] Huber PJ (1964): Robust estimation of a location parameter, *Annals of Statistics*, 53, 73-101.

[17] Ramachandran P, Zoph B, Le QV (2017): Searching for activation functions, arXiv:1710.05941.

[18] LeCun Y, Bottou L, Orr GB, Muller KR (1998): Efficient BackProp, In: Orr GB, Muller KR (eds.) Neural Networks: Tricks of the Trade. Lecture Notes in Computer Science, 1524.

